

ALiSNet: Accurate and Lightweight Human Segmentation Network for Fashion E-Commerce

Amrollah Seifoddini¹ ^a, Koen Vernooij¹, Timon Künzle¹, Alessandro Canopoli¹, Malte Alf¹, Anna Volokitin¹ and Reza Shirvany²

¹Zalando SE, Switzerland

²Zalando SE, Germany

Keywords: On-Device, Human-Segmentation, Privacy-Preserving, Fashion, e-Commerce.

Abstract: Accurately estimating human body shape from photos can enable innovative applications in fashion, from mass customization, to size and fit recommendations and virtual try-on. Body silhouettes calculated from user pictures are effective representations of the body shape for downstream tasks. Smartphones provide a convenient way for users to capture images of their body, and on-device image processing allows predicting body segmentation while protecting users' privacy. Existing off-the-shelf methods for human segmentation are closed source and cannot be specialized for our application of body shape and measurement estimation. Therefore, we create a new segmentation model by simplifying Semantic FPN with PointRend, an existing accurate model. We finetune this model on a high-quality dataset of humans in a restricted set of poses relevant for our application. We obtain our final model, ALiSNet, with a size of 4MB and $97.6 \pm 1.0\%$ mIoU, compared to Apple Person Segmentation, which has an accuracy of $94.4 \pm 5.7\%$ mIoU on our dataset.

1 INTRODUCTION

Human segmentation has emerged as foundational to applications across a diverse range from autonomous driving to social media, virtual and augmented reality, and online fashion. In the case of online fashion, giving users a way to easily capture their body shape is valuable, since it can be used to recommend appropriate clothing sizes or to enable virtual try-on. However, to determine the right size and fit of clothing, the body shape needs to be determined with very high accuracy in order to be of value. For example, in an image of 2k resolution in height, a segmentation error of two pixels on the boundary can change a measurement such as chest circumference by 10mm. Users' body shape can be more accurately determined if they wear tight-fitting clothes, making it even more important than in other applications to preserve privacy. Hence, mobile human segmentation is a good fit for fashion applications, as images can be both captured and processed on-device.

In this paper we propose an approach to achieve an accurate and lightweight human segmentation method for these applications. Although off-the-shelf mobile human segmentation methods are available, such

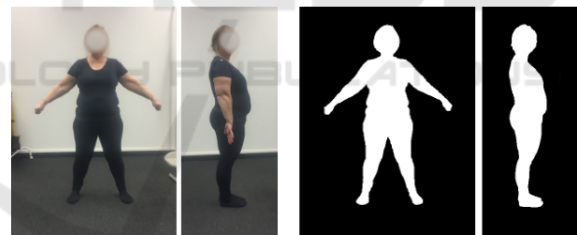


Figure 1: Ground truth body annotations. The boundary in particular is critical for body shape prediction.

as Apple Person Segmentation (Apple,) and Google MLKit's BlazePose (Bazarevsky et al., 2020), these methods are closed-source and cannot be adapted to our task to achieve the required accuracy. Instead, we design a model based on Semantic FPN with PointRend for our task.

Crucial to the success of our method is finetuning on a task specific dataset of user-taken photos in front and side views, as shown in Figure 1. Orthogonal views such as this are commonly used in various anthropometry setups, e.g. (Smith et al., 2019). Such silhouettes can be used to model the 3D body shape of users, as proposed in (Dibra et al., 2016; Dibra et al., 2017; Smith et al., 2019) or to directly predict measurements (Yan et al., 2021) for fashion applications. While relying on the large body of publicly available

^a  <https://orcid.org/0000-0002-6757-3175>

data for the segmentation task, we augment it by using a small yet specific dataset of 6147 high resolution images with highly accurate annotations to overcome the limitations of publicly available data.

Our main contributions are thus two-fold: First, we demonstrate that a relatively small set of high-quality annotations can boost segmentation accuracy. Second, we simplify a large and high quality baseline method, Semantic FPN (Kirillov et al., 2019) with PointRend refinement (Kirillov et al., 2020) with a few steps to achieve almost the same performance with $100\times$ model size. The main changes to the original model are: exchanging the backbone with a modified version of the mobile-optimized MnasNet (Tan et al., 2019), using quantization-aware training, and removing network components that we found not to be contributing to segmentation accuracy. Our final **Accurate and Lightweight mobile human Segmentation Network (ALiSNet)**, achieves 97.6% mIoU and is 4MB in size, where an off-the-shelf method such as BlazePose-Segmentation achieves 93.7% mIoU on our data, with a 6MB model, and Apple Person Segmentation achieves 94.4% mIoU. It was not possible to fine-tune either of these models to our data as they are closed-sourced. Additionally, ALiSNet’s accuracy is only marginally lower than the 97.8% mIoU achieved by the 350 MB baseline.

2 RELATED WORK

The categories of methods most relevant to our work in the domain of on-device human segmentation are portrait editing, video call background effects, and general-purpose real time whole body segmentation methods.

Many portrait editing predict alpha mattes, which are masks that allow blending foreground and background regions. In this application, having accurate segmentation of textures such as wisps of hair is very important. Google Pixel’s alpha matting method (Orts-Escolano and Ehman, 2022) relies on data collected using a custom volumetric lighting setup. Apple Person Segmentation (Apple,) in *accurate* mode also belongs to this category of methods. However, such accuracy on the texture level is not necessary for our application. Besides, most existing alpha matting methods are trained only on faces.

Real-time portrait segmentation methods for video calls focus on segmenting the human upper body. ExtremeC3Net (Park et al., 2019) and SiNet (Li et al., 2020) are examples of models that achieve very good performance under a parameter count of 200K.

There are also several methods focused on real-time segmentation of the whole body. One example is Google MLKit BlazePose-Segmentation (Bazarevsky et al., 2020) which relies on correct prediction of body bounding box. (Strohmayr et al., 2021) focuses on reducing latency for general purpose human segmentation. (Liang et al., 2022) introduces Multi-domain TriSeNet Networks for the real-time single person segmentation for photo-editing applications. (Xi et al., 2019) uses saliency map derived from accurate pose information to improve segmentation accuracy especially in multi-person scenes.

(Han et al., 2020) categorizes the set of techniques for reducing model size into *model compression* and *compact model design* methods. Although we make use of quantization-aware training (Wu et al., 2015) in this paper, which is a compression technique, we mostly take advantage of compact model components. These include compact networks that can be used as feature extractors, such as MnasNet (Tan et al., 2019), FBNet (Wu et al., 2019a) and MobileNetV3 (Howard et al., 2019) which have been found using Neural Architecture Search.

We recommend the related work section of (Knapp, 2021) for a more extensive review of works related to mobile person segmentation.

Finally, our work can be used in downstream applications for estimating body shape. This is an active research area, with several approaches of estimating body shape from silhouette, such as (Song et al., 2018; Song et al., 2016; Ji et al., 2019; Dibra et al., 2016).

Datasets. We review several datasets with permissive licenses that include person segmentation labels. These include MS COCO (Lin et al., 2014), shown in Figure 2, LVIS (Gupta et al., 2019) (contains higher quality annotations for COCO images), Google Open Images (Kuznetsova et al., 2018). There are limitations with each of these datasets. COCO annotations are based on polygons and therefore not accurate around the object boundaries. LVIS annotations are very accurate and dense in each image but they are not



Figure 2: An example image and annotation from the COCO dataset. Note the low accuracy of the polygon annotation.

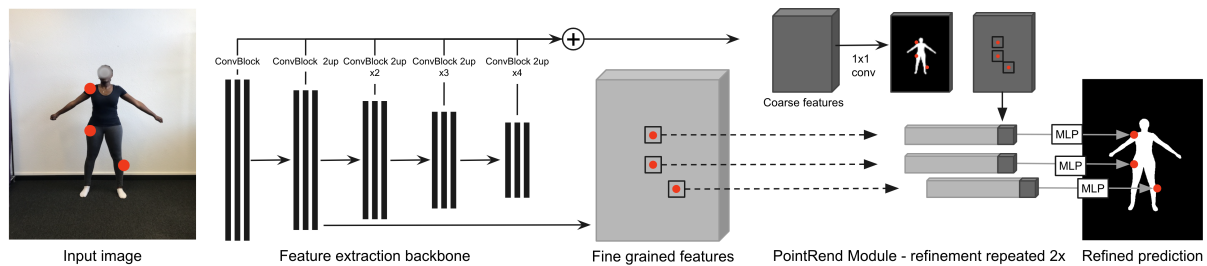


Figure 3: ALiSNet Architecture. The first stage of our method is the feature extractor backbone which produces features at 5 resolution levels. These features are convolved and added together to form the coarse features. The coarse features are projected to a coarse segmentation using a 1×1 convolution. Uncertain points on the coarse segmentation mask are selected and refined using PointRend. During a PointRend refinement step, coarse predictions and finegrained features from these locations are concatenated and fed to an MLP to obtain refined segmentation predictions. This refinement is repeated two times. In the diagram, *ConvBlock* is a conv, batch-norm, ReLu sequence and *2up* is a 2x bi-linear upsampling.

yet available for the entire COCO dataset, especially in the human category where only around 1.8k images are annotated. Finally, the Google Open Images dataset is sparse in segmentation coverage in each image compared to COCO, as many object instances are not segmented yet.

3 METHOD

3.1 Model

Our model, ALiSNet, is a version of Semantic FPN with PointRend (Kirillov et al., 2020), simplified for on-device use. We chose Semantic FPN with PointRend as a baseline because of its high accuracy in segmenting object boundaries. In theory, other baseline methods could also be used to show the effectiveness of our approach.

Semantic FPN with PointRend. Semantic FPN first extracts features using a backbone and further process them with a Feature Pyramid Network (FPN) (Lin et al., 2017a). Then, a coarse segmentation map is computed from the aggregated coarse features. PointRend then samples uncertain points on the coarse segmentation and concatenates fine-grained features from the FPN with the coarse predictions at each location and uses this as an input to a classifier to refine the prediction at this location.

Changes to Baseline for On-Device Use. In this work, we use three approaches to address the problem of reducing the model size while preserving segmentation accuracy. First, we take advantage of a mobile feature extraction backbone to replace the ResNeXt101 (Xie et al., 2017) feature extractor in our baseline. Second, we quantize our model using

quantization-aware training, allowing us to replace 32bit floating point parameters with equivalent int8 representations. We choose to use quantization aware training as opposed to post-training quantization as it is known to lead to more accurate results. Third, we replace the feature pyramid network used in the original model with a simpler aggregation step, skipping the FPN top-down path. The final ALiSNet architecture is shown in Figure 3.

Training Loss. Our training loss includes the segmentation loss between the predicted and ground-truth labels, and the PointRend loss. For the segmentation loss, we experimented with cross-entropy and focal loss (Lin et al., 2017b), and found cross-entropy to be more stable during training. We therefore used the latter for further trainings. The PointRend loss is taken from the reference implementation of PointRend in detectron2 and contains the sum of cross-entropies between predicted and ground-truth labels of all points refined during the refinement process for each sample in the mini-batch.

3.2 Data

An important element in making our approach successful is to pre-train on a large-scale coarsely annotated dataset and fine-tune on a high-quality specific dataset.

Pretraining on COCO. Following other segmentation methods (Kirillov et al., 2020) we base our work on MS COCO. Out of all images in COCO, we only use those containing at least one person (around 60k images). The COCO default annotation format is designed for instance segmentation. Thus, we merge the segmentation masks of human instances in each image to create corresponding segmentation masks for semantic segmentation.

Small Scale In-House Dataset. We observe that even though object instance coverage in COCO is very high, there are disadvantages when using only that data for our task: Segmentation annotations are not pixel accurate since the objects are annotated using polygons. The scale of objects can be extremely diverse, ranging from objects of 10 pixels in height to objects covering almost the entire image. The diversity of human poses and occlusions is extreme and most images contain only a small body part or crowds of people. This is helpful for general segmentation tasks but our experiments show that it limits the accuracy of on-device models in more controlled tasks such as body shape estimation where pose, viewing angle and scale of the body does not vary much.

To overcome these limitations of large-scale general purpose datasets, we make use of a small high-quality dataset focused on enabling accurate human body segmentation for our task. To build this complementary dataset, we use an in-house mobile app with interactive video features to guide the users to stand in the correct front and side view poses at the right distance to be fully in the frame. The app was made available for both iOS and Android, powered by real-time pose estimation models native to the OS. Images are taken with portrait (vertical) framing format. The calculated pose-keypoints are available for the captured images and can be used in downstream tasks too. To protect participants' privacy, the images were cropped around the bounding box containing the person. The bounding boxes are calculated from predicted pose-keypoints in the app and enlarging the box by 10% margin on each side. This dataset includes 6147 images which are randomly distributed in train/validation/test splits with 60/20/20% ratios respectively. The number of front and side view images is almost balanced, and the ratio of male/female participants is 45/55%. The annotation is performed by an expert annotation team, and the quality of segmentation masks was checked by two quality expert groups. An example of this data is shown in Figure 4.

4 EXPERIMENTAL SETUP

4.1 Implementation Details

For this paper, we used the detectron2 framework (Wu et al., 2019b) built on top of PyTorch, which includes the reference implementation of PointRend.

On the mobile side, the model is executed by the PyTorch Mobile interpreter to facilitate the deployment of developed models. To that end, the model is first converted by the TorchScript compiler and the



Figure 4: Left: Examples of front and side view images in the target poses. Ground-truth annotation masks are overlaid with green color onto the pictures.

resulting model graph is loaded by the mobile interpreter. Because the iterative PointRend head contains control flows based on the input, we have to use scripting instead of tracing for computation graph generation. Scripted models are not fully optimized for runtime, therefore the performance sometimes is lower than traced models. For the quantization of the model we use the QNNPACK (Dukhan et al., 2020) backend which is optimized for ARM CPUs available in mobile devices.

4.2 Model Training

As described in subsection 3.2, we augment training our models on COCO with fine-tuning on our in-house dataset. We also experiment with CNN backbones that are pre-trained on ImageNet (Deng et al., 2009) classification tasks. All experiments are done in machines in Amazon AWS with 4 V100 GPUs totalling 128 GB graphic memory. The mini-batch size of training is set to 8 for large models (e.g. ResNeXt101 backbone) and 16 for smaller backbones (i.e. MnasNet, MobileNet, FBNet). The base learning rate is set to 0.01 for the case of batch-size = 8 and 0.02 for batch-size = 16 following the recommendation of a linearly scaling learning rate (Goyal et al., 2017). During training we augment the data using default augmentation tools provided by detectron2. This includes random resizing, horizontal flip, color jitter and brightness and saturation change. The range of sizes for the shorter side of image in resizing is set randomly from a predefined list (between 120 and 800) while keeping the longer side under 1024 and the scale-factor between 0.5 and 4. This prevents too much down-sampling of our high-resolution images during training.

For the fine-tuning step, as a standard practice we experimented with freezing the first N ($N \leq 2$) stages of the backbone to improve generalization of the model and avoid over-fitting but we have observed

Table 1: Effect of each model change step on the accuracy and size of model. mIoU values are reported as mean \pm std in percent.

Model configuration	Size (MB)	mIoU
ResNeXt101 + FPN-SemSeg + PointRend	351.7	97.8 \pm 1.0
Replace ResNeXt101 with MnasNet-B1	52.0	97.7 \pm 0.9
Quantization-Aware-Training	12.9	97.7 \pm 0.9
Remove FPN-top-down path (ALiSNet)	4.0	97.6 \pm 1.0
Google MLKit (BlazePose-Segmentation)-accurate	27.7	93.9 \pm 5.3
Google MLKit (BlazePose-Segmentation)-balanced	6.4	93.7 \pm 5.9
Apple Person Segmentation (accurate)	-	94.3 \pm 5.9
Apple Person Segmentation (balanced)	-	94.4 \pm 5.7

Table 2: Effect of fine-tuning on our dataset. First mIoU column: results after training on COCO only. second mIoU column: result after fine-tuning on our dataset. (Q) indicates the model is quantized using quantization-aware-training.

Model	Size (MB)	mIoU with COCO	mIoU with fine-tuning
ResNeXt101 + FPN-SemSeg + PointRend	351.7	94.0 \pm 3.8	97.8 \pm 1.0
MobileNetV3 + FPN-SemSeg + PointRend	35.1	91.2 \pm 6.2	97.7 \pm 1.1
(Q) MnasNet-B1 + SemSeg + PointRend (ALiSNet)	4.0	90.0 \pm 6.8	97.6 \pm 0.9

that not freezing any layer can improve the generalization results in our case. We also experimented with reducing the learning-rate by $\times 10$ for the fine-tuning step compared to the pre-training learning rate. However, we found that the model converged quicker and to better results when we did not reduce the learning rate.

4.3 Evaluation

We evaluate our models with mean Intersection Over Union (mIoU) which is defined in Equation 1. This metric is in the $[0, 1]$ range and then reported as percentage.

$$mIoU = \frac{1}{N} \sum_{i=1}^N \frac{|pred_i \cap GT_i|}{|pred_i \cup GT_i|} \times 100 \quad (1)$$

where $pred$ and GT are the prediction and ground-truth segmentation masks of sample i respectively. During evaluation, images are sized to 1024 on height after cropping them to the person bounding box.

5 EXPERIMENTAL RESULTS

In this section, first we explore the effect of different aspects of our model. Then we do a quantitative and qualitative comparison of our method with two other related person-segmentation methods.

5.1 Effect of Model Design Choices

Reduction of Size of Components: As shown in Table 1, starting from the baseline model (351.7MB), we first obtain a model size of 52.0MB by replacing the ResNeXt101 feature backbone with MnasNet, saving around 300 MB. Then we applied Quantization Aware Training, which further shrinks the model size by $\times 4$, resulting in 12.9MB, as we replace 32 bit floating point with int8 representation.

We then show that the top-down branch of FPN which combines high-level semantic features with low-level features can be removed from the model with only 0.1% reduction in accuracy. We argue that in our model, PointRend carries the job of merging high-level and low-level features, thus making the top-down path of FPN mostly redundant. Furthermore, scale of persons in our data does not vary enough to require FPN-top-down features.

Fine-Tuning. We first train all the models on the COCO person class. In Table 2, we show the effect of fine-tuning these models on our high-quality task-specific dataset. It is clear that the fine-tuning significantly improves the mIoU, and the effect is greater for smaller models.

PointRend. Although the PointRend module adds to the 0.2MB size and 20% to the runtime of our method, we use it, as Table 3 shows that it adds around 0.3% mIoU to the model accuracy.

Table 3: Effect of PointRend on accuracy of Semantic FPN without and with PointRend. Both models are quantized.

Backbone	FBNetV3	MnasNet-B1
no PR	97.4 ± 1.1	97.4 ± 1.0
With PR	97.7 ± 0.9	97.7 ± 0.9

CNN Backbones Choice. We compared the effect using MobileNetV3 (Howard et al., 2019), MnasNet (Tan et al., 2019), FBNetV3 (Dai et al., 2021) as mobile-friendly backbone feature extractors. Table 4 shows that all of the mobile feature extractors have around the same performance in our task, which is only 0.1% lower than the much larger ResNeXt101. We chose to use MnasNet due to lower variance and its availability in the the torchvision framework.

Table 4: Effect of different CNN backbones on accuracy of the Semantic FPN segmentation model.

Model backbone	mIoU
ResNeXt101	97.8 ± 1.0
MobileNetV3	97.7 ± 1.1
(Q) FBNetV3	97.7 ± 0.9
(Q) MnasNet-B1	97.7 ± 0.9

5.2 Runtime on Mobile Devices

We evaluated our model on a set of real mobile devices provided by the AWS Device Farm¹. The distribution of runtime is shown in Figure 5. For this evaluation, 90 high-resolution images from the dataset are processed using our in-house evaluation mobile app. Images are resized to 2k resolution in height while preserving the aspect ratio and then cropped to the person bounding box. The cropped images are passed to the model, where they are resized to 1024 in height internally before segmentation. As the bounding box of the person varies between images, a significant variance of the runtime on a single device can be noticed. On recent iPhones the model runs well below 1s and for an older Android phone like the Moto G4 the mean is around 8s. In iPhone SE and Galaxy S21 there are some outliers in runtime, for reasons we were not able to determine. The model is running on CPU mode due to limited support of PyTorch for mobile-GPU in quantized models.

5.3 Comparison to BlazePose and Apple Person Segmentation

We compare with two on-device person segmentation methods.

¹<https://aws.amazon.com/device-farm/>

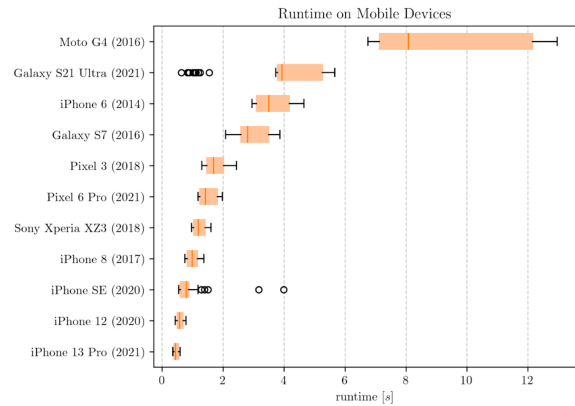


Figure 5: Runtime on mobile devices. Our method runs in less than two seconds on most modern devices. As of October 2022, iPhone 13 is the latest iPhone available on the Amazon Device Farm.

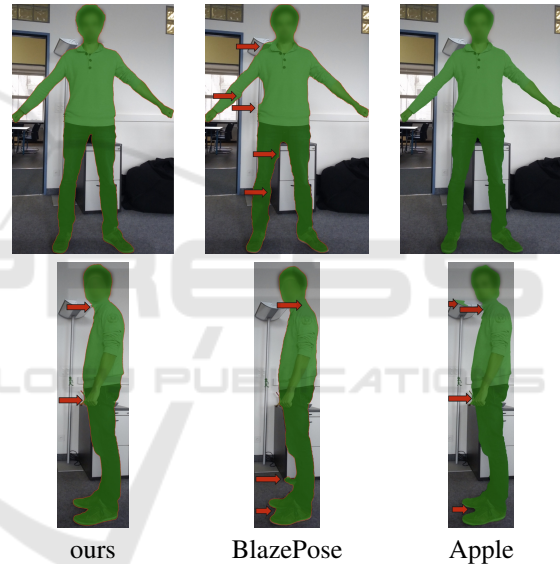


Figure 6: Comparison of segmentation methods. Red arrows indicate mis-segmented regions. In these images, the threshold for the Apple segmentation algorithm (balanced) was set to 0.6 to obtain the best results. In the quantitative evaluation, the value is 0.3.

BlazePose (Bazarevsky et al., 2020) is a on-device real-time body pose tracking method, which provides a segmentation prediction option. We compare two settings of the BlazePose model, balanced and accurate, which have model sizes of 6.4MB and 27.7MB respectively.

We also compare to Apple Person Segmentation which was made available in iOS15. Information about the details of this model is not available.

The output segmentation maps of these methods are probabilistic, and need to be thresholded to compute the final binary silhouette maps. Thresholds

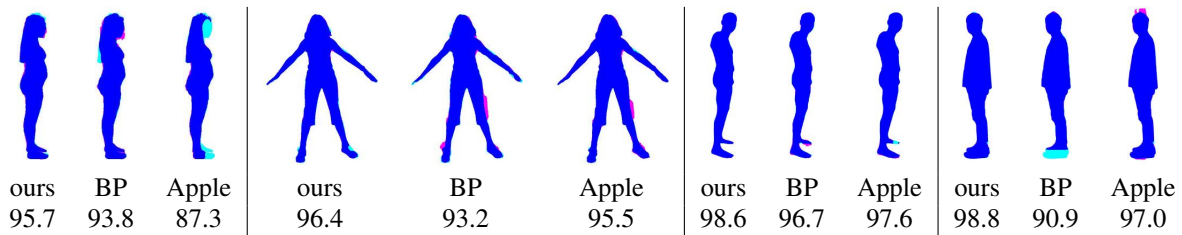


Figure 7: Overlays of predicted segmentations over the ground truth annotations, blue intersection, from our in-house dataset, from our method, BlazePose (BP) and Apple, with the IoU. We ranked the images in the test set by their their mIoUs using AlisNet, and displayed the 5th, 10th, 90th and 95th-% images in this ranking. As the photos are confidential, we show only the silhouettes here. After data collection, all images were anonymized using face-blur, which is seen in the Apple Segmentation in the first image. In one of the BP segmentations you can see the issue of bounding box prediction cutting out part of the feet.

were determined using a sweep of values and were set to 0.5 for BlazePose and 0.3 for Apple.

It is not possible to fine-tune either of these methods on our data.

As seen in Table 1, both BlazePose and Apple Segmentations have a much lower mIoU than AlisNet on our dataset, while having a much higher standard deviation. This indicates that fine-tuning on our data allows our model to avoid certain mistakes in segmentation. Neither of the compared methods are designed for the use-case of segmentation for accurate human body measurement. BlazePose is optimized for real-time pose estimation, which means it lies on a different point of the performance-accuracy trade-off. Apple Person Segmentation is designed to power Portrait Mode. Segmentation examples from all three methods are shown in Figure 6. In the front view, both our method and Apple produce more accurate segmentations than BlazePose. In the side view, we see that all three methods have difficulty with background objects, and that the Apple method produces artifacts in the lamp.

Figure 7 shows overlays from the test set of our dataset. In this figure we show both “bad” and “good” segmentations from our model, however, we see that our segmentation has a higher IoU than the other methods, as we have trained our model on this dataset.

6 DISCUSSION

We presented a method for accurate mobile human segmentation along with a set of general steps that can be used to simplify existing large-scale models for on-device applications.

Although our model handles most images well, there are cases with confusing background textures where our method and other methods fail, as shown in Figure 8. Other challenging conditions include dim lighting, dark shadows or other image distortions. Improving the performance under these con-

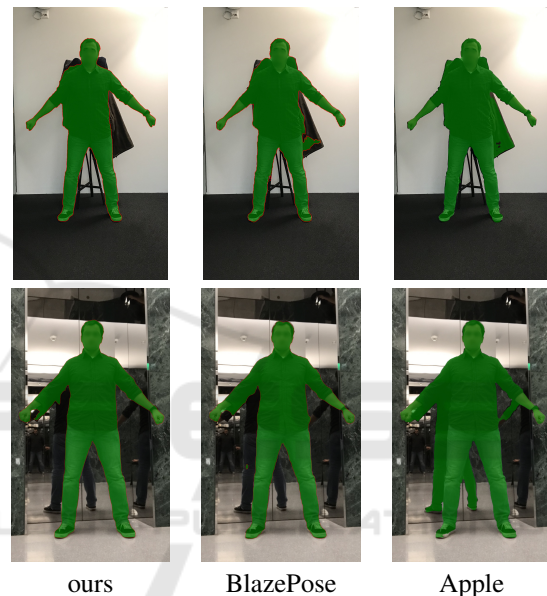


Figure 8: Examples of failure cases for segmentation algorithms. In our user collected dataset, people take pictures at home, and sometimes have clothes (top) or mirrors (bottom) in the background, which cause the segmentation method to not work correctly. This is a shortcoming of all the methods we evaluate here.

ditions would be an important future direction.

In the future we will be experimenting with on-device segmentation models for accurate body shape and measurement estimation.

ACKNOWLEDGEMENTS

We would like to thank Julia Friberg for her contributions in evaluation of the models on real mobile phones.

REFERENCES

- Apple. Applying Matte Effects to People in Images and Video.
- Bazarevsky, V., Grishchenko, I., Raveendran, K., Zhu, T., Zhang, F., and Grundmann, M. (2020). BlazePose: On-device real-time body pose tracking. *CoRR*, abs/2006.10204.
- Dai, X., Wan, A., Zhang, P., Wu, B., He, Z., Wei, Z., Chen, K., Tian, Y., Yu, M., Vajda, P., et al. (2021). Fbnetv3: Joint architecture-recipe search using predictor pre-training. In *Proceedings of the IEEE/CVF Conference on Computer Vision and Pattern Recognition*, pages 16276–16285.
- Deng, J., Dong, W., Socher, R., Li, L.-J., Li, K., and Fei-Fei, L. (2009). Imagenet: A large-scale hierarchical image database. In *2009 IEEE conference on computer vision and pattern recognition*, pages 248–255. Ieee.
- Dibra, E., Jain, H., Öztireli, C., Ziegler, R., and Gross, M. (2016). Hs-nets: Estimating human body shape from silhouettes with convolutional neural networks. In *2016 fourth international conference on 3D vision (3DV)*, pages 108–117. IEEE.
- Dibra, E., Jain, H., Öztireli, C., Ziegler, R., and Gross, M. (2017). Human shape from silhouettes using generative hks descriptors and cross-modal neural networks. In *Proceedings of the IEEE conference on computer vision and pattern recognition*, pages 4826–4836.
- Dukhan, M., Wu, Y., and Lu, H. (2020). Qnnpack: open source library for optimized mobile deep learning. <https://github.com/pytorch/QNNPACK>.
- Goyal, P., Dollár, P., Girshick, R. B., Noordhuis, P., Wesolowski, L., Kyrola, A., Tulloch, A., Jia, Y., and He, K. (2017). Accurate, large minibatch SGD: training imagenet in 1 hour. *CoRR*, abs/1706.02677.
- Gupta, A., Dollár, P., and Girshick, R. B. (2019). LVIS: A dataset for large vocabulary instance segmentation. *CoRR*, abs/1908.03195.
- Han, K., Wang, Y., Tian, Q., Guo, J., Xu, C., and Xu, C. (2020). Ghostnet: More features from cheap operations. In *Proceedings of the IEEE/CVF conference on computer vision and pattern recognition*, pages 1580–1589.
- Howard, A., Sandler, M., Chu, G., Chen, L.-C., Chen, B., Tan, M., Wang, W., Zhu, Y., Pang, R., Vasudevan, V., et al. (2019). Searching for mobilenetv3. In *Proceedings of the IEEE/CVF International Conference on Computer Vision*, pages 1314–1324.
- Ji, Z., Qi, X., Wang, Y., Xu, G., Du, P., Wu, X., and Wu, Q. (2019). Human body shape reconstruction from binary silhouette images. *Computer Aided Geometric Design*, 71:231–243.
- Kirillov, A., Girshick, R., He, K., and Dollar, P. (2019). Panoptic feature pyramid networks. In *Proceedings of the IEEE/CVF Conference on Computer Vision and Pattern Recognition (CVPR)*.
- Kirillov, A., Wu, Y., He, K., and Girshick, R. (2020). Pointrend: Image segmentation as rendering. In *Proceedings of the IEEE/CVF conference on computer vision and pattern recognition*, pages 9799–9808.
- Knapp, J. (2021). *Real-Time Person Segmentation on Mobile Phones*. PhD thesis, Wien.
- Kuznetsova, A., Rom, H., Alldrin, N., Uijlings, J. R. R., Krasin, I., Pont-Tuset, J., Kamali, S., Popov, S., Mallocci, M., Duerig, T., and Ferrari, V. (2018). The open images dataset V4: unified image classification, object detection, and visual relationship detection at scale. *CoRR*, abs/1811.00982.
- Li, Y., Luo, A., and Lyu, S. (2020). Fast portrait segmentation with highly light-weight network. In *2020 IEEE International Conference on Image Processing (ICIP)*, pages 1511–1515. IEEE.
- Liang, Z., Guo, K., Li, X., Jin, X., and Shen, J. (2022). Person foreground segmentation by learning multi-domain networks. *IEEE Transactions on Image Processing*, 31:585–597.
- Lin, T.-Y., Dollár, P., Girshick, R., He, K., Hariharan, B., and Belongie, S. (2017a). Feature pyramid networks for object detection. In *Proceedings of the IEEE conference on computer vision and pattern recognition*, pages 2117–2125.
- Lin, T.-Y., Goyal, P., Girshick, R., He, K., and Dollár, P. (2017b). Focal loss for dense object detection. In *Proceedings of the IEEE international conference on computer vision*, pages 2980–2988.
- Lin, T.-Y., Maire, M., Belongie, S., Bourdev, L., Girshick, R., Hays, J., Perona, P., Ramanan, D., Zitnick, C. L., and Dollár, P. (2014). Microsoft coco: Common objects in context. cite arxiv:1405.0312Comment: 1) updated annotation pipeline description and figures; 2) added new section describing datasets splits; 3) updated author list.
- Orts-Escolano, S. and Ehman, J. (2022). Accurate Alpha Matting for Portrait Mode Selfies on Pixel 6 . <https://ai.googleblog.com/2022/01/accurate-alpha-matting-for-portrait.html>.
- Park, H., Sjöstrand, L. L., Yoo, Y., and Kwak, N. (2019). Extremec3net: Extreme lightweight portrait segmentation networks using advanced c3-modules. *arXiv preprint arXiv:1908.03093*.
- Smith, B. M., Chari, V., Agrawal, A., Rehg, J. M., and Sever, R. (2019). Towards accurate 3d human body reconstruction from silhouettes. In *2019 International Conference on 3D Vision (3DV)*, pages 279–288. IEEE.
- Song, D., Tong, R., Chang, J., Yang, X., Tang, M., and Zhang, J. J. (2016). 3d body shapes estimation from dressed-human silhouettes. In *Computer Graphics Forum*, volume 35, pages 147–156. Wiley Online Library.
- Song, D., Tong, R., Du, J., Zhang, Y., and Jin, Y. (2018). Data-driven 3-d human body customization with a mobile device. *IEEE Access*, 6:27939–27948.
- Strohmayr, J., Knapp, J., and Kampel, M. (2021). Efficient models for real-time person segmentation on mobile phones. In *2021 29th European Signal Processing Conference (EUSIPCO)*, pages 651–655. IEEE.

- Tan, M., Chen, B., Pang, R., Vasudevan, V., Sandler, M., Howard, A., and Le, Q. V. (2019). Mnasnet: Platform-aware neural architecture search for mobile. In *Proceedings of the IEEE/CVF Conference on Computer Vision and Pattern Recognition*, pages 2820–2828.
- Wu, B., Dai, X., Zhang, P., Wang, Y., Sun, F., Wu, Y., Tian, Y., Vajda, P., Jia, Y., and Keutzer, K. (2019a). Fbnet: Hardware-aware efficient convnet design via differentiable neural architecture search. In *Proceedings of the IEEE/CVF Conference on Computer Vision and Pattern Recognition*, pages 10734–10742.
- Wu, J., Leng, C., Wang, Y., Hu, Q., and Cheng, J. (2015). Quantized convolutional neural networks for mobile devices. arxiv eprints, page. *arXiv preprint arXiv:1512.06473*.
- Wu, Y., Kirillov, A., Massa, F., Lo, W.-Y., and Girshick, R. (2019b). Detectron2. <https://github.com/facebookresearch/detectron2>.
- Xi, W., Chen, J., Lin, Q., and Allebach, J. P. (2019). High-accuracy automatic person segmentation with novel spatial saliency map. In *2019 IEEE International Conference on Image Processing (ICIP)*, pages 1560–1564.
- Xie, S., Girshick, R., Dollár, P., Tu, Z., and He, K. (2017). Aggregated residual transformations for deep neural networks. In *Proceedings of the IEEE conference on computer vision and pattern recognition*, pages 1492–1500.
- Yan, S., Wirta, J., and Kämäräinen, J.-K. (2021). Silhouette body measurement benchmarks. In *2020 25th International Conference on Pattern Recognition (ICPR)*, pages 7804–7809. IEEE.